HHS Public Access

Author manuscript

J Med Chem. Author manuscript; available in PMC 2019 February 22.

Published in final edited form as:

J Med Chem. 2018 October 11; 61(19): 8895–8907. doi:10.1021/acs.jmedchem.8b01136.

Optimization of a Series of Mu Opioid Receptor (MOR) Agonists with High G Protein Signaling Bias

Nicole M. Kennedy[#†,‡], **Cullen L. Schmid**[#‡], **Nicolette C. Ross**[†,‡], **Kimberly M. Lovell**[†,‡], **Zhizhou Yue**[†,‡], **Yen Ting Chen**[†,‡], **Michael D. Cameron**[‡], **Laura M. Bohn**[*,‡], and **Thomas D. Bannister**[*,†,‡]

[†] Department of Chemistry, The Scripps Research Institute, Jupiter, Florida 33458, United States

[‡] Department of Molecular Medicine, The Scripps Research Institute, Jupiter, Florida 33458, United States

[#] These authors contributed equally to this work.

Abstract

While mu opioid receptor (MOR) agonists are especially effective as broad-spectrum pain relievers, it has been exceptionally difficult to achieve a clear separation of analgesia from many problematic side effects. Recently, many groups have sought MOR agonists that induce minimal β-arrestin-mediated signaling because MOR agonist-treated β-arrestin2 knockout mice were found to display enhanced antinociceptive effects with significantly less respiratory depression and tachyphylaxis. Substantial data now exists to support the premise that G protein signaling biased MOR agonists can be effective analgesic agents. We recently showed that, within a chemical series, the degree of bias correlates linearly with the magnitude of the respiratory safety index. Herein we describe the synthesis and optimization of piperidine benzimidazolone MOR agonists that together display a wide range of bias (G/β-arr2). We identify structural features affecting potency and maximizing bias and show that many compounds have desirable properties, such as long half-lives and high brain penetration.

Graphical Abstract:

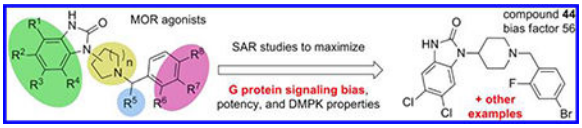

[*]**Corresponding Authors:** For T.D.B., medicinal chemistry issues: phone, (561)228-2206; tbannister@scripps.edu, For L.M.B., pharmacology studies: phone, (561)228-2227; lbohn@scripps.edu.

Author Contributions

The manuscript was written through contributions of all authors. All authors have given approval to the final version of the manuscript.

The authors declare no competing financial interest.

Supporting Information

The Supporting Information is available free of charge on the ACS Publications website at DOI: 10.1021/acs.jmedchem.8b01136.

Synthetic procedures and characterization details of additional compounds, molecular strings, ^{1}H NMR spectra of key compounds that were used for in vivo studies (PDF)

Molecular formula strings (CSV)

INTRODUCTION

Agonists of the mu opioid receptor (MOR), such as morphine and fentanyl, are extensively used for the treatment of moderate to severe pain due to their high efficacy;[1] however, the dose required to achieve adequate pain relief often elicits multiple unwanted side effects, including respiratory suppression, constipation, and tolerance. The respiratory suppressive effect of opioids is especially concerning, as it is the root cause of death by opioid overdose, which claimed more than 40000 victims in the USA in 2016.[2]The identification and development of safer analgesic agents may play an important role in combatting the opioid epidemic.

The most effective opioid pain relievers are agonists of the MOR.[3] As with all G protein coupled receptors (GPCRs), agonist binding to MOR initiates the dissociation of heterotrimeric G protein subunits and the activation of subsequent downstream signaling. The MOR also interacts with βarrestins, scaffolding and regulatory proteins with multifaceted roles, including receptor desensitization of the G protein cascades and the facilitation of receptor internalization and signaling that can be distinct from G protein mediated responses.[4] Studies using βarrestin2 knockout (βarr2-KO) mice strongly suggest that the interaction between MOR and βarrestin2 produces many of morphine's undesirable effects in vivo.[5–10] In the βarr2-KO mice, morphine retained its analgesic properties, yet, in comparison to wildtype littermates, constipation, tolerance, and respiratory suppression were largely attenuated.[5–8,10] The basis of this work is to test the hypothesis that a MOR agonist capable of activating G protein signaling without prompting the engagement of βarrestins will separate analgesia from many of the adverse effects that arise downstream of MOR activation.

The ability of a compound to stimulate one signaling pathway over another upon engaging the receptor is referred to "functional selectivity" or "biased agonism."[4,11–14] Compounds that preferentially activate G protein signaling over βarrestin2 recruitment in the MOR have been developed by a number of groups.[15–19] Two reported clinical trials with TRV130 (aka Oliceridine) demonstrate that one such G protein biased MOR agonist has analgesic efficacy with a modest improvement in respiratory suppression compared to morphine.[20,21] These clinical results suggest that imparting G coupling bias in MOR agonists may lead to the discovery and eventual availability of opioid analgesic agents with improved safety, especially if the magnitude of signaling bias is augmented so that more than a modest improvement in therapeutic index may be achieved.

We recently disclosed members of a family of substituted piperidine benzimidazolone MOR agonists with high affinity for the MOR (0.3–14 nM), high G protein signaling bias (up to 100-fold bias relative to DAMGO in some assays), and high selectivity for MOR over the other opioid receptors.[22] The modular design of the core scaffold permitted extensive structural diversification, an important advantage because we found that only a small subset of potential analogues in the series display significant G protein signaling bias. We have optimized these MOR agonists for potency, G protein signaling bias, and drug-like properties. Our objective has been to identify compounds with morphine-like efficacy in vivo (or better) that would not induce respiratory suppression at, or even well above, an

efficacious dose. Within a set of related compounds, we achieved this goal and demonstrated that the degree of signaling bias within the series linearly correlated to the magnitude of protection from respiratory suppression.[22] Given that slight structural changes can greatly impact signaling bias, understanding the structural features favoring alternative MOR signaling pathways could greatly enhance efforts to identify new safe and efficacious analgesic agents.

Herein, we report the first comprehensive bias-focused structure–activity relationship (SAR) study for this class of MOR agonists. We systematically varied the R^1–R^8 substituents of the generalized N-benzyl cycloamino benzimidazolone scaffold as well as varied the ring size in the central saturated ring, which in most cases is a piperidine (Figure 1).

Many structural changes were found to markedly impact the properties of MOR agonists. The iterative design and evaluation of analogues drove the optimization of G protein signaling potency, the deselection of β-arrestin interactions, and the optimization of desirable drug-like properties, such as a suitable half-life, lack of cytochrome P450 (CYP) inhibition, and high blood–brain barrier (BBB) permeability. Signaling bias was characterized using separate cell-based assays designed to measure G protein coupling and β-arrestin2 recruitment. Bias was quantitated by applying the operational model,[23] which measures the affinity, potency, and efficacy of the compound in each assay relative to the reference full agonist [D-Ala^2, NMe-Phe^4, Gly-ol^5]-enkephalin (DAMGO) and then allows for comparison across assays.[11,23] For optimized biased analogues, we measured various in vitro parameters, such as liver microsome stability and CYP inhibition, then followed up with in vivo studies for metabolic stability and BBB permeability. Results from these in vitro and in vivo studies advance our understanding of the chemical properties that underlie MOR signaling bias and may aid the development of additional promising leads separating analgesic activity from unwanted, and potentially deadly, respiratory suppression.

RESULTS AND DISCUSSION

Synthesis.

As shown in Scheme 1, a general five-step synthetic route was used to synthesize the majority of the benzimidazolone derivatives[24] (compounds with a central piperidine ring are shown; see Scheme S1, Supporting Information, for an alternate route). In the general procedure, nucleophilic aromatic substitution of a fluoronitrobenzene starting material with *N*-Boc-4-aminopiperidine (or in some cases with a homologue having a 5- or 7-membered ring) was followed by nitro group reduction of **I**, cyclic urea formation of **II**, Boc deprotection of **III**, and finally, either direct alkylation or reductive amination of **IV** produced the desired analogues. Reductive amination used an aldehyde (R^5 = H) or ketone (R^5 = Me or Et). The products were isolated and characterized in free base form, unless indicated, and then were evaluated in all biological and pharmacological assays as either the free base or as the mono mesylate salt.

Structure–Activity Relationships.

In these SAR studies, substituents R^1−R^8 were varied, as was the size of the central ring (Figure 1). Each analogue was screened for its ability to activate G protein coupling at MOR using the standard ^{35}S-GTPγS binding assay in membranes from CHO-K1 cells expressing the human MOR. βarrestin2 recruitment profiles to the human MOR were determined using a cell-based commercially available enzyme-fragment complementation assay (EFC). In both assays, full dose response curves for the test compound were run in parallel to the reference full agonist, DAMGO, as previously described.[22] To quantitatively compare the differences observed between the two signaling assays, the operational model was used to calculate $\Delta\Delta\log(\tau/K_A)$ values, with confidence intervals and bias factors (the antilog of $\Delta\Delta\log(\tau/K_A)$).[22,23] A bias factor of 1 ($\Delta\Delta\log(\tau/K_A)$ value of 0) indicates that the compound is unbiased relative to DAMGO. A bias factor less than 1 ($\Delta\Delta\log(\tau/K_A)$ value less than 0) indicates bias toward βarrestin2 recruitment over GTPγS binding, while a bias factor greater than 1 ($\Delta\Delta\log(\tau/K_A)$ value greater than 0) indicates bias toward GTPγS binding over βarrestin2 recruitment. Additionally, we used morphine as a clinically relevant opioid analgesic for comparison purposes. In these assays, we found morphine, with a bias factor of 1.8, to show a slight bias toward G protein coupling over βarrestin2 recruitment compared to DAMGO. Safer analgesic agents would be expected to have significantly higher levels of G protein coupling bias.[22]

As shown in Table 1, the parent *N*-benzyl piperidine 4-benzimidazolone (**1**), with all substituents R^1−R^8 = H, had modest potency in the GTPγS assay (EC_{50} = 2.2 μM) but was a full agonist (E_{MAX} = 78% of DAMGO). Compound **1** performed similar to DAMGO in both assays (GTPγS/βarr2 bias factor = 0.9). After exploring the impact of various R^6−R^8 substituents on the *N*-benzyl ring, we found that the addition of an *ortho*-Cl (**2**) or *para*-Cl substituent (**4**)[22] improved potency. The *ortho*-Cl substituent also imparted a modest G protein signaling bias (GTPγS/βarr2 bias factor = 2.5).

Many *para*-substituted analogues (**4–7**) were similar in potency and efficacy in the GTPγS assay (EC_{50} = 367−591 nM, E_{MAX} = 68–88%) and were similarly unbiased (GTPγS/βarr2 bias factors = 0.9−1.2). *para*-Substituted analogues (**8–10**) were less potent and/or efficacious in the GTPγS assay compared to **4–7**, with **10** showing no significant activity until the 10 μM concentration. The *meta*-substituted compounds **3**, **11**, and **12** were also less potent and less efficacious in the GTPγS assay in comparison to their *para*-substituted counterparts, with compound **11** acting as a partial GTPγS agonist (E_{MAX} = 33% of DAMGO). When a second Cl substituent was added to the *para* position (**13**), the GTPγS potency and efficacy was reduced further and the potency at βarrestin2 was outside the experimental range of the assay. Thus, *ortho* and *para* substituted *N*-benzyl analogues were of greatest interest in this series from the perspective of obtaining biased agonists of useful potency. The potential for combining the *ortho* and *para* effects was demonstrated with compounds **14** and **15**, in which **14** is a potent full agonist showing some bias for G protein signaling (EC_{50} = 152 nM, E_{MAX} = 93%, GTPγS/βarr2 bias factor = 3.8).

As shown in Table 2, adding an *N*-benzylic methyl group (R^5 = Me) substantially increased potency in the parent racemic compound (**16**, EC_{50} = 102 nM)[22] as compared to **2** but had

little effect on GTPγS/βarr2 bias. Analogous to the Table 1 series, the addition of an *ortho*- or *para*-Cl substituent further augmented potency (EC_{50} = 31 and 16 nM, respectively). In this case, the *para*-Cl compound **18**[22] was more biased than was the *ortho*-Cl compound **17**. The boost in GTPγS potency and efficacy eroded when an ethyl rather than a methyl group was present (**19**).

Replacement of the *para*-Cl substituent with either *para*-F substituent (**20**) or *para*-OMe group (**22**) gave potent compounds but with reduced bias; however, replacement with either a *para*-Br substituent (**21**) or *para*-OCF_3 group (**26**), increased GTPγS/βarr2 bias to 4.1 and 8.3, respectively. Increasing the size of the alkoxy group to ethoxy (23), iso-propoxy (**24**), or ethylene dioxy (**25**)[22] eroded potency in the GTPγS assay; however, the GTPγS/βarr2 bias factor of **24** was modestly increased to 3.6. Compounds **20** and **25**, interestingly, promoted bias toward βarrestin2 recruitment, opposite of what is expected to provide analgesia with reduced side effects (GTPγS/βarr2 bias factors = 0.56 and 0.47, respectively). We previously observed βarrestin2 bias for fentanyl vs DAMGO at the human MOR when comparing GTPγS binding and the βarrestin2 recruitment using the enzyme fragment complementation assays (as used in this current study, GTPγS/βarr2 bias factor = 0.18, measured relative to DAMGO)[22] and drew correlations with a reduced therapeutic index comparing mouse hot plate responses to changes in arterial oxygen saturation. Compound **25**, aka SR-11501, shared similar profiles with fentanyl in both the in vivo and in vitro assays,[22] and thus, it is attractive to speculate that preference for βarrestin2 recruitment over G protein coupling in vitro will consistently indicate a very narrow respiratory safety index in vivo. Compounds such as **20** and additional compounds across a range of bias factors will allow further testing of this hypothesis. Finally, compounds **27** and **28** showed that the addition of an *ortho*-F substituent had little effect on the potency, efficacy, and bias of compounds having *para*-Cl (**18**) and *para*-Br (**21**) substituents.

We then investigated the effect of varying benzimidazolone substituents R^1–R^4 (see Table 3). In this study, for consistency in interpretation, we held the distal *N*-benzyl substituent constant as an *ortho*-Cl (R^6 = Cl). Compounds with a Cl at R^1(**29**), R^2(**30**), or R^3 (**31**) were full agonists with increased GTPγS potency, GTPγS efficacy, and GTPγS/βarr2 bias relative to the *des*-Cl analogue **2.** Compound **32**, with R^4 = Cl, however, was far less active. The near-complete lack of potency for compounds **30** and **31** in the βarrestin2 recruitment assay (EC_{50} > 10 μM) was encouraging and led us to explore whether groups other than Cl might also deselect βarrestin2 recruitment. Thus, we studied compounds with various R^2 substituents (**33–39**) and found that the groups shown erode GTPγ potency and/or GTPγS/βarr2 bias, except for compound **33**, R^2 = Me, which was similar in potency and efficacy in the GTPγ assay but was slightly less biased due to the higher potency in the βarrestin2 recruitment assay (EC_{50} = 6.8 μM). We concluded that a chloro substituent in the benzimidazolone ring system (R^1, R^2, or R^3 = Cl) favors higher potency and efficacy in the GTPγS assay while giving substantial bias (i.e., minimal βarrestin2 recruitment).

To determine if the benzimidazolone chloro effect was compatible with substituents other than *ortho*-Cl on the distal *N*-benzyl ring, as well as to evaluate compatibility with a benzylic methyl at R^5 (which was expected to increase potency, as was shown in Table 2), another diverse series of analogues was investigated (Table 4). This set of compounds

contained, in the *N*-benzyl ring, *ortho*-Fand *para*-Br substituents at R^6 and R^8, respectively, because this combination had given advantages in potency and bias (see Table 2, compare **17** and **27**).

Compared to compound **15**, with R^1–R^5 = H, the presence of Cl at R^1 (**40**), R^2 (**41**), or R^3 (**42**) had little effect on potency in the GTPγS assay, but bias was more pronounced, especially in compound **41** (GTPγ/βarr2 bias factor = 23, Table 4). Potency in the GTPγS assay was greatly augmented, as noted earlier (Table 2), with the addition of a benzylic methyl group at R^5: see compounds **15** and **27**, while bias was relatively unchanged. Di- and trichlorinated analogues were also prepared. A Cl present at both R^1 and R^3 (**43**) had no advantage over the reference compound **15** with regard to potency in G protein signaling or in bias disfavoring βarrestin2 recruitment. On the other hand, a Cl at both R^2 and R^3 (**44**), while similar in potency to compound **15** in the GTPγS signaling assay (EC_{50} = 91 nM), was essentially devoid of all βarrestin2 recruitment activity (EC_{50} > 10 μM, E_{MAX} = 12% of DAMGO, GTPγ/βarr2 bias factor = 56). As expected based upon earlier data for compound **32**(Table 3), a Cl at R^4 is not tolerated; thus, the trichloro compound **45** lost potency in the GTPγS assay.

The potency and bias effects for the compound series in Table 4 are made even more apparent when comparing full dose–response curves, as shown in Figure 2. Moving clockwise within the figure, part A shows curves for the GTPγS binding assay (circles) and the βarrestin2 recruitment assay (squares) for the modestly biased reference compound **15** (green) compared with DAMGO (white). Part B shows the potency enhancement seen for **27**, which has a benzylic methyl group: note the left-shifted curve (red circles). Part C shows data for the monochloro substituted compound **41**, which is less potent because it lacks a benzylic methyl group but is still highly biased. Part D shows data for compound **43**, the less biased and less potent dichloro benzimidazolone analogue. Part E shows the enhanced signaling bias of compound **44**; note the flattened βarrestin2 curve (blue squares). The right-shifted curve (dark-blue circles) in part F depicts the significantly less potent compound **45**. It is worth noting that at the highest concentrations tested, in some cases we see an increase in response; however, we are unable to determine if the response would plateau, as solubility limitations preclude higher concentrations in the assay. Therefore, in the tables, % maximum stimulation at 10000 nM is provided when potency cannot be calculated. Finally, part G graphically compares the analogues and depicts the substantial signaling bias seen for compounds **41** and **44** (GTPγ/βarr2 bias factors = 23 and 56, respectively).

With the finding that compound **44**, with R^2 = R^3 = Cl, has the greatest bias among Table 4 analogues, we then held this portion of the structure constant and also held the substitution pattern in the distal *N*-benzyl ring constant, with a *para*-Br substituent, which we had shown to confer βarrestin2 bias (see compound **15** in Table 1 and compound **21** in Table 2). The additional *ortho*-F substituent in Table 4 analogues had only a small effect; compare compound **44**(Table 4) to compound **46** (Table 5). With both ends of the molecule held constant, we probed the effect of changing the size of the central ring as well as altering where the benzimidazolone is attached (Table 5). The 7-membered (**47**) and 5-membered ring analogues (**48** and **49**) were less potent in the GTPγS assay and were less biased

relative to the corresponding 4-substituted piperidine (**46**, EC_{50} = 149 nM and GTPγS/βarr2 bias factor = 45).[22] Furthermore, the 3-substituted piperidines (**50** and **51**) were essentially inactive as MOR agonists, with no significant efficacy until tested at the 10 μM concentration.

Drug Metabolism and Pharmacokinetics (DMPK) Properties.

For a compound to advance into further development, it must be metabolically stable and must have suitable tissue distribution (including, in this case, high brain exposure). Furthermore, compounds must be nontoxic at efficacious doses and must not prompt drug–drug interactions. As a preliminary gauge of compound metabolic stability, we assessed the stability of promising compounds in the presence of mouse and human liver microsomes. To determine the potential for drug–drug interactions, we studied their ability to inhibit four of the major metabolizing cytochrome P450 (CYP) isoforms. This in vitro DMPK data was used, along with the GTPγSpotency and GTPγS/βarr2 bias data, to select compounds for further PK evaluation in vivo.

Table 6 shows selected in vitro and in vivo properties of many compounds in the series that were chosen for follow-up due to their significant GTPγS potency (EC_{50} < 400 nM) and high bias (GTPγS/βarr2 bias factor >5). An exception is compound **25**, which was used as a comparator. This compound, like fentanyl,[22] is βarrestion2 biased (relative to DAMGO) and thus is expected to have enhanced respiratory suppressive effects that could limit its usefulness. In this series, the inhibition of CYP isoforms was not a major concern: among the compounds tested, only compound **29** gave >50% inhibition of any CYP isoform at 10 μM. The liver microsome stability of these compounds was more widely variable. Fortunately, human liver microsome stability exceeding 1 h was seen in some of the compounds (**26, 41, 44,** and **46**).Though these compounds were generally less stable to mouse liver microsomes compared to the human, stability was sufficient for in vivo PK evaluations in mice. Of note, we previously reported that the G protein and βarrestin2 signaling profiles for two compounds in this series (**25** and **46**) are consistent between the mouse and human MOR.[22]

To determine if our MOR agonists could penetrate the BBB, which is required in an opioid analgesic agent, compound **25** and the compounds most highly biased toward GTPγS over βarr2 (**41**, **44**, and **46**) were administered intraperitoneally (ip) at 6 mg/kg[22] and brain levels were determined after 1 h. As shown in Table 6, these compounds were present in the brain 1 h following systemic injection at levels exceeding that seen with a systemic injection of morphine at the same dose. High brain levels at this time point are consistent with enhanced compound stability as indicated by liver microsome stability data, suggesting the value of using in vitro DMPK assessments to drive the selection of compounds for in vivo evaluation.

CONCLUSIONS

In analyzing data for the set of 51 related compounds shown in Tables 1–5, as well as DMPK and efficacy properties (Table 6 and Figure 2), we have established a pharmacophore for G protein biased MOR agonism. Certain hydrophobic substituents, especially halogen atoms in the distal benzimidazolone and the *N*-benzyl ring, are essential for extreme G

protein coupling bias, relative to DAMGO. The presence of a central piperidine ring is also preferred. In many cases, a benzylic methyl group augments potency and has a small but typically beneficial impact upon bias. The structural basis for these effects is currently under investigation. Additional ongoing studies include: more extensive target selectivity profiling of top compounds, safety studies, antinociceptive studies in multiple species, and the separation and/or the stereoselective asymmetric synthesis of individual isomers of analogues reported here as racemates (e.g., Table 2 compounds). Because the degree of respiratory safety correlates linearly with the magnitude of the GTPγS/βarr2 bias factor as calculated herein,[22] we hope that the trends noted in this SAR study may guide the design of substantially safer opioid analgesic agents.

EXPERIMENTAL SECTION

General Procedures.

Materials were purchased from commercial vendors and used without purification. All moisture-sensitive reactions were performed under argon. Experiments were monitored by LCMS or TLC and visualized using an ultraviolet lamp (254 nm) or staining with $KMnO_4$. Flash column chromatography was performed using a Teledyne ISCO Combiflash Rf+ and Luknova silica gel cartridges. All NMR data was collected at room temperature on a Brüker Ultrashield 400 MHz nuclear magnetic resonance spectrometer. Chemical shifts for ^{1}H NMR spectra are reported in parts per million (ppm) relative to residual solvent signal as an internal standard: DMSO (δ 2.50), $CHCl_3$ (δ 7.26), or MeOH (δ 3.31). Multiplicities are given as s (singlet), d (doublet), t (triplet), q (quartet), or m (multiplet). Coupling constants are reported as a *J* value in hertz (Hz). Mass spectra were recorded on a Thermo Scientific 3000 LCQ Fleet system (ESI) using a Discovery HS C18 HPLC column (10 cm × 2.1 mm, 5 μm) at 35 °C with UV detection at 210, 254, and 280 nm. Flow rate was 0.7 mL/min using a solvent gradient of 5–95% B over 4 min (total run time = 6 min), where A = 0.1% formic acid in water and B = 0.1% formic acid in acetonitrile. Analytical HPLC was performed on an Agilent 1100 series using an Agilent Eclipse XDB-C18 HPLC column (4.6 mm × 150 mm, 5 μm) with UV detection at 254 nm. Flow rate was 1.75 mL/min using a solvent gradient of 10–90% B over 8 min (total run time = 10 min), where A = 0.1% TFA and 1% acetonitrile in water and B = acetonitrile. The purity of all compounds used in the bioassays was determined to be ≥95% by analytical HPLC. For the in vitro studies, DAMGO (Tocris) and morphine sulfate pentahydrate (NIDA Drug Supply Program) were dissolved in water as 10 mM stocks. All other compounds were dissolved in 100% DMSO as 10 mM stocks. For all assays, the final DMSO concentration was 1%.

tert-Butyl 4-((2-Nitrophenyl)amino)piperidine-1-carboxylate (I).[22]—A mixture of 1-fluoro-2-nitrobenzene (0.5 mL, 5.0 mmol), *N*-boc-4-aminopiperidine (1.0 g, 5.0 mmol), K_2CO_3 (0.8 g, 5.9 mmol), and DMSO (5 mL) was stirred at room temperature overnight under argon. The reaction mixture was quenched with water, and the aqueous layer was extracted with CH_2Cl_2; the combined organic layers were dried over Na_2SO_4 and concentrated to dryness. Purification afforded pure product I(1.5 g, 93% yield). ^{1}H NMR (400 MHz, $CDCl_3$) δ 8.17 (dd, *J* = 8.6, 1.8 Hz, 1H), 8.08 (d, *J* = 1.6 Hz, 1H), 7.42 (td, *J* =

7.8, 1.6 Hz, 1H), 6.86 (d, *J* = 8.4 Hz, 1H), 6.64 (td, *J* = 7.8, 1.2 Hz, 1H), 4.01 (dt, *J* = 13.6, 3.8 Hz, 1H), 3.70−3.64 (m, 1H), 3.04 (td, *J* = 12.2, 3.0 Hz, 2H).

tert-Butyl 4-((2-Aminophenyl)amino)piperidine-1-carboxylate (II).[22]—A 50% aqueous suspension of Raney nickel (11.9 mL) was added to a mixture of **I** (1.5 g, 4.7 mmol) in absolute EtOH (95 mL). Hydrazine hydrate (2.3 mL, 47 mmol) was then added dropwise. The mixture was heated to 45 °C, stirred for 10 min, and then filtered through a pad of Celite. The pad was washed with MeOH, and the filtrate was concentrated to dryness. Purification afforded pure product **II** (1.0 g, 74% yield). ^{1}H NMR (400 MHz, $CDCl_3$) δ 6.79 (td, *J* = 7.2, 2.2 Hz, 1H), 6.72−6.66 (m, 3H), 4.14−4.02 (m, 1H), 3.41−3.34 (m, 4H), 2.93 (t, *J* = 11.8 Hz, 2H), 2.00 (dd, *J* = 13.0, 3.0 Hz, 2H), 1.48 (s, 9H), 1.36 (qd, *J* = 12.2, 4.0 Hz, 2H). MS(*m*/*z*): [M + H] calcd for $C_{16}H_{26}N_3O_2$ 292.19, found 291.76.

tert-Butyl 4-(2-Oxo-2,3-dihydro-1H-benzo[d]imidazol-1-yl)-piperidine-1-carboxylate (III).[22]—CDI (780 mg, 4.8 mmol) was slowly added to a solution of **II**(1.0 g, 3.4 mmol) in THF (30 mL). The reaction mixture was stirred overnight at room temperature under argon and then quenched with 10% HCl. The aqueous layer was extracted with EtOAc. The combined organic layers were dried over Na_2SO_4 and concentrated to dryness. Purification afforded pure product **III** (0.6 g, 55% yield). ^{1}H NMR (400 MHz, $CDCl_3$) δ 9.30 (s, 1H), 7.16−7.06 (m, 4H), 4.48 (tt, *J* = 12.6, 4.0 Hz, 1H), 4.33 (dd, *J* = 11.6, 2.0 Hz, 2H), 2.88 (td, *J* = 13.0, 2.4 Hz, 2H), 2.34 (qd, *J* = 12.8, 4.4 Hz, 2H), 1.84 (dd, *J* = 12.0, 2.4 Hz, 2H), 1.51 (s, 9H). MS(*m*/*z*): [M + H] calcd for $C_{17}H_{24}N_3O_3$ 318.17, found 317.71.

1-(Piperidin-4-yl)-1H-benzo[d]imidazol-2(3H)-one TFA Salt (IV).[22]—Compound **III** (0.6 g, 1.9 mmol) was dissolved in a 33% solution of TFA in CH_2Cl_2 (6 mL). The reaction mixture was stirred at room temperature until completion and then was concentrated to dryness. The solid was dissolved in 1:1 water/acetonitrile. The solution was frozen and then subjected to lyophilization overnight giving **IV** in the form of a TFA salt. This material was used without further purification. ^{1}H NMR (400 MHz, CD_3OD) δ 7.29−7.26 (m, 1H), 7.11−7.08 (m, 3H), 4.55 (tt, *J* = 12.2, 4.2 Hz, 1H), 3.58 (dt, *J* = 12.8, 2.2 Hz, 2H), 3.22 (td, *J* = 13.2, 2.4 Hz, 2H), 2.74 (qd, *J* = 12.6, 4.4 Hz, 2H), 2.06 (dd, *J* = 12.8, 1.6 Hz, 2H). MS(*m*/*z*): [M + H] calcd for $C_{12}H_{16}N_3O$ 218.12, found 217.92.

1-(1-(Benzyl)piperidin-4-yl)-1H-benzo[d]imidazol-2(3H)-one (1).[25]—A mixture of **IV** (free base, 110 mg, 0.5 mmol), benzyl bromide (87 mg, 0.5 mmol), DIPEA (132 μL, 0.8 mmol), and DMF (1 mL) was stirred at room temperature overnight under argon. Upon completion, the solvent was removed under reduced pressure, and the residue was dissolved in EtOAc (20 mL). This reaction mixture was washed with saturated $NaHCO_3$ followed by brine. The organic layer was dried over Na_2SO_4 and concentrated to dryness. Purification afforded pure product **1** (139 mg, 89% yield). ^{1}H NMR (400 MHz, $(CD_3)_2SO$) δ 10.82 (s, 1H), 7.35−7.34 (m, 4H), 7.28−7.21 (m, 1H), 7.01−6.95 (m, 3H), 4.14 (tt, *J* = 12.4, 4.0 Hz, 1H), 3.53 (s, 2H), 2.94 (d, *J* = 11.6 Hz, 2H), 2.35 (qd, *J* = 12.4, 4.0 Hz, 2H), 2.09 (t, *J* = 11.0 Hz, 2H), 1.64 (d, *J* = 9.2 Hz, 2H). MS(*m*/*z*): [M + H] calcd for $C_{19}H_{22}N_3O$ 308.17, found 308.06. HPLC t_R = 3.39 min.

GTPγS Binding.

MOR-stimulated GTPγS binding was determined in membranes prepared from CHO-hMOR cells as described.[22] CHO-hMOR cells were serum-starved for 30 min and collected via gentle scraping in EDTA buffer. Membranes were then prepared via dounce homogenization and centrifugation at 20000g for 30 min at 4 °C. GTPγS binding reactions were performed in 200 μL volumes containing 10 μg of CHO-hMOR membranes, 50 μM guanosine-5″-diphosphate (GDP, Sigma-Aldrich G7127), 0.1 nM ^{35}S-GTPγS (PerkinElmer NEG030H), and concentrations of the compounds ranging from 0.1 nM to 10 μM were incubated for 1 h at room temperature. Reactions were terminated by rapid filtration through GF/B glass fiber filter plates (PerkinElmer), and radioactivity was counted with a TopCount NXT scintillation counter (PerkinElmer).

βarrestin2 Enzyme Fragment Complementation Assay.

USOS-βarrestin-hMOR-PathHunter cells (DiscoveRx 93–0213C3) were used to determine βarrestin2 interactions with the MOR by an enzyme fragment complementation assay.[22] The cells (4000 cells/ well) were incubated with 0.1 nM to 10−31 μM (depending on compound solubility) concentrations of the test compounds at 37 °C for 90 min, and βarrestin2 translocation was determined according to the manufacturer's instructions (DiscoveRx). Luminescence was measured using a SpectraMax M5^{e} microplate reader (Molecular Devices) with 1 s integration times.

Pharmacokinetic Parameters.

To determine stability in hepatic microsomes, compound (1 μM) was incubated with 1 mg/mL human or mouse hepatic micosomes at 37 °C with continuous shaking.[26] At 0, 5, 10, 20, 40, and 60 min time points, aliquots were removed and acetonitrile was added to quench the reactions and precipitate the proteins. Samples were then centrifuged though 0.45 μm filter plates and half-lives were determined by LC-MS/MS.

To determine cytochrome P450 inhibition, 1 μM compound was incubated with human liver microsomes and selective marker substrates (1A2, phenacetin demethylation to acetaminophen; 2C9, tolbutamide hydroxylation to hydroxytolbutamide; 2D6, bufuralol hydroxylation to 4′-hydroxybufuralol; 3A4, midazolam hydroxylation to 1′-hydroxymidazolam). After a 10 min incubation, the reaction was terminated and the percent inhibition was determined.[27]

Pharmacokinetics in Mice.—Male C57BL6/J mice were purchased from Jackson Laboratory (Bar Harbor, ME) and assessed at 10−12 weeks per age. All mice were used in accordance with the National Institutes of Health Guidelines for the Care and Use of Laboratory Animals with approval by the Scripps Research Institutional Animal Care and Use Committee (IACUC). To determine brain penetrance, mice were injected with drug (ip at mg/kg at 10 μL/g volumes mouse body weight using a vehicle of 1:1:8 DMSO, Tween 80, and purified water). Mice were sacrificed by cervical dislocation 1 h following drug treatment, and isolated brains were flash frozen in liquid nitrogen. Drug levels were determined using a LC-MS operated in positive-ion mode, 1 h after treatment.

Data and Statistical Analysis.

GraphPad Prism (v. 7.0) was used for data and statistical analysis. All data are presented as mean ± SEM or with 95% confidence intervals, as indicated in the figure and table legends. For the in vitro studies, the assays were run in duplicate, with at least three independent replicates and DAMGO was run as the reference compound in every experiment for normalization. EC_{50} and E_{MAX} values were calculated by nonlinear (three parameter) regression analysis. Because of the limit of solubility for some compounds, E_{MAX} values are reported at 10 μM concentrations in instances where the data did not converge or where potency values were outside the linear experimental range of the assay.

Analysis of Bias.—Bias factors were calculated according to the operational model using DAMGO as the reference agonist. As in the prior article, the conservative constraint was applied to the operational model to fit the K_A value to fall between 0 and 10^{-15} M to allow for curve fitting in the absence of reaching a maximum plateau in one of the responses; the $\Delta\log(\tau/K_A)$ values relative to DAMGO were constrained to be less than 10.[22,27]

Supplementary Material

Refer to Web version on PubMed Central for supplementary material.

ACKNOWLEDGMENTS

This project is supported by NIH grant R01DA033073 (to L.M.B. and T.D.B.) and R01DA038694 (to L.M.B.). The authors have filed for patent protection for the compounds described herein.

ABBREVIATIONS USED

BBB	blood–brain barrier
Boc	*tert*-butyloxycarbonyl
CDI	1,1-carbonyldiimidazole
CH_2Cl_2	methylene chloride
CYP	cytochrome P450
DAMGO	[D-Ala^2, NMe-Phe^4, Gly-ol^5]-enkephalin
DIPEA	*N,N*-diisopropylethylamine
DMPK	drug metabolism and pharmacokinetics
DMSO	dimethylsulfoxide
EC_{50}	half-maximal effective concentration
E_{MAX}	maximal efficacy
EFC	enzyme fragment complementation
EtOH	ethanol

GPCR	G protein-coupled receptor
HPLC	high pressure liquid chromatography
ip	intraperitoneally
H_2NNH_2	hydrazine
K_2CO_3	potassium carbonate
kg	kilogram
$KMnO_4$	potassium permanganate
KO	knockout
mg	milligram
LC/MS	liquid chromatography mass spectrum
MOR	mu opioid receptor
$NaBH_3CN$	sodium cyanoborohydride
$NaBH(OAc)_3$	sodium triacetoxyborohydride
Ni	nickel
nm	nanometer
nM	nanomolar
NMR	nuclear magnetic resonance
PK	pharmacokinetics
^{35}S-GTPγS	G protein-coupling assay
SAR	structure–activity relationship
TFA	trifluoroacetic acid
TLC	thin layer chromatography
THF	tetrahydrofuran
μM	micromolar
μg	microgram

REFERENCES

(1). (a)Morgan MM; Christie MJ Analysis of Opioid Efficacy, Tolerance, Addiction and Dependence from Cell Culture to Human. Br. J. Pharmacol 2011, 164, 1322–1334. [PubMed: 21434879] (b)Melnikova I Pain Market. Nat. Rev. Drug Discovery 2010, 9, 589–590. [PubMed: 20651743]

(2). (a)Seth P; Scholl L; Rudd RA; Bacon S Overdose Deaths Involving Opioids, Cocaine, and Psychostimulants-United States, 2015–2016. MMWR Morb. Mortal Wkly. Rep 2018, 67, 349–

358. [PubMed: 29596405] (b)Frank RG; Pollack HA Addressing the Fentanyl Threat to Public Health. N. Engl. J. Med 2017, 376, 605–607. [PubMed: 28199808]

(3). (a)Feng Y; He X; Yang Y; Chao D; Lazarus LH; Xia Y Current Research on Opioid Receptor Function. Curr. Drug Targets 2012, 13, 230–246. [PubMed: 22204322] (b)Dahan A; Sarton E; Teppema L; Olievier C; Nieuwenhuijs D; Matthes HW; Kieffer BL Anesthetic Potency and Influence of Morphine and Sevoflurane on Respiration in Mu-Opioid Receptor Knockout Mice. Anesthesiology 2001, 94, 824–832. [PubMed: 11388534] (c)Matthes HW; Maldonado R; Simonin F; Valverde O; Slowe S; Kitchen I; Befort K; Dierich A; LeMeur M; Dollé P; Tzavara E; Hanoune J; Roques BP; Kieffer BL Loss of Morphine-induced Analgesia, Reward Effect and Withdrawal Symptoms in Mice lacking the Mu-Opioid Receptor Gene. Nature 1996, 383, 819–823. [PubMed: 8893006]

(4). Luttrell LM; Maudsley S; Bohn LM Fulfilling the Promise of “Biased” G Protein-Coupled Receptor Agonism. Mol. Pharmacol 2015, 88, 579–588. [PubMed: 26134495]

(5). Raehal KM; Walker JK; Bohn LM Morphine Side Effects in Beta-arrestin2 Knockout Mice. J. Pharmacol. Exp. Ther 2005, 314, 1195–1201. [PubMed: 15917400]

(6). Bu H; Liu X; Tian X; Yang H; Gao F Enhancement of Morphine Analgesia and Prevention of Morphine Tolerance by Downregulation of Beta-arrestin2 with Antigene RNAs in Mice. Int. J. Neurosci 2015, 125, 56–65. [PubMed: 24555516]

(7). Bohn LM; Lefkowitz RJ; Gainetdinov RR; Peppel K; Caron MG; Lin FT Enhanced Morphine Analgesia in Mice lacking Beta-arrestin2. Science 1999, 286, 2495–2498. [PubMed: 10617462]

(8). Li Y; Liu X; Liu C; Kang J; Yang J; Pei G; Wu C Improvement of Morphine-mediated Analgesia by Inhibition of Beta-arrestin2 Expression in Mice Periaqueductal Gray Matter. Int. J. Mol. Sci 2009, 10, 954–963. [PubMed: 19399231]

(9). Raehal K; Groer CE; Schmid CL; Bohn LM Functional Selectivity at the Mu-Opioid Receptor: Implications for Understanding Opiate Analgesia and Tolerance. Pharmacol. Rev 2011, 63, 1001–1019. [PubMed: 21873412]

(10). Bohn LM; Gainetdinov RR; Lin FT; Lefkowitz RJ; Caron MG Mu-Opioid Receptor Desensitization by Beta-arrestin2 determines Morphine Tolerance but not Dependence. Nature 2000, 408, 720–723. [PubMed: 11130073]

(11). Kenakin T; Watson C; Muniz-Medina V; Christopoulos A; Novick S A Simple Method for Quantifying Functional Selectivity and Agonist Bias. ACS Chem. Neurosci 2012, 3, 193–203. [PubMed: 22860188]

(12). Urban JD; Clarke WP; von Zastrow M; Nichols DE; Kobilka B; Weinstein H; Javitch JA; Roth BL; Christopoulos A; Sexton PM; Miller KJ; Spedding M; Mailman RB Functional Selectivity and Classical Concepts of Quantitative Pharmacology. J. Pharmacol. Exp. Ther 2007, 320, 1–13. [PubMed: 16803859]

(13). Rankovic Z; Brust TF; Bohn LM Biased agonism: An Emerging Paradigm in GPCR Drug Discovery. Bioorg. Med. Chem. Lett 2016, 26, 241–250. [PubMed: 26707396]

(14). Wisler JW; Xiao K; Thomsen ARB; Lefkowitz RJ Recent Developments in Biased Agonism. Curr. Opin. Cell Biol 2014, 27, 18–24. [PubMed: 24680426]

(15). Groer CE; Tidgewell K; Moyer RA; Harding WW; Rothman RB; Prisinzano TE; Bohn LM An Opioid Agonist that does not Induce Mu-Opioid Receptor–Arrestin Interactions or Receptor Internalization. Mol. Pharmacol 2007, 71, 549–557. [PubMed: 17090705]

(16). DeWire SM; Yamashita DS; Rominger DH; Liu G; Cowan CL; Graczyk TM; Chen XT; Pitis PM; Gotchev D; Yuan C; Koblish M; Lark MW; Violin JD A G Protein-Biased Ligand at the μ-Opioid Receptor is Potently Analgesic with Reduced Gastrointestinal and Respiratory Dysfunction compared with Morphine. J. Pharmacol. Exp. Ther 2013, 344, 708–717. [PubMed: 23300227]

(17). Kruegel AC; Gassaway MM; Kapoor A; Váradi A; Majumdar S; Filizola M; Javitch JA; Sames D Synthetic and Receptor Signaling Explorations of the Mitragyna Alkaloids: Mitragynine as an Atypical Molecular Framework for Opioid Receptor Modulators. J. Am. Chem. Soc 2016, 138, 6754–6764. [PubMed: 27192616]

(18). Manglik A; Lin H; Aryal DK; McCorvy JD; Dengler D; Corder G; Levit A; Kling RC; Bernat V; Hübner H; Huang XP; Sassano MF; Giguére PM; Löber S; Duan D; Scherrer G; Kobilka BK;

Gmeiner P; Roth BL; Schoichet BK Structure-based Discovery of Opioid Analgesics with Reduced Side Effects. Nature 2016, 537, 185–190. [PubMed: 27533032]

(19). Crowley RS; Riley AP; Sherwood AM; Groer CE; Shivaperumal N; Biscaia M; Paton K; Schneider S; Provasi D; Kivell BM; Filizola M; Prisinzano TE Synthetic Studies of Neoclerodane Diterpenes from *Salvia divinorum*: Identification of a Potent and Centrally Acting μ-Opioid Analgesic with Reduced Abuse Liability. J. Med. Chem 2016, 59, 11027–11038. [PubMed: 27958743]

(20). Soergel DG; Subach RA; Burnham N; Lark MW; James IE; Sadler BM; Skobieranda F; Violin JD; Webster LR Biased Agonism of the Mu-Opioid Receptor by TRV130 Increases Analgesia and Reduces On-target Adverse Effects versus Morphine: A Randomized, Double-blind, Placebo-controlled, Crossover Study in Healthy Volunteers. Pain 2014, 155, 1829–1835. [PubMed: 24954166]

(21). Singla N; Minkowitz H; Soergel D; Burt D; Skobieranda F Respiratory Safety Signal with Oliceridine (TRV130), a Novel Mu Receptor G Protein Pathway Selective Modulator (Mu-GPS), vs Morphine: a Safety Analysis of a Phase 2b Randomized Clinical Trial. J. Pain 2016, 17, S82.

(22). Schmid CL; Kennedy NM; Ross NC; Lovell KM; Yue Z; Morgenweck J; Cameron MD; Bannister TD; Bohn LM Bias Factor and Therapeutic Window Correlate to Predict Safer Opioid Analgesics. Cell 2017, 171, 1165–1175. [PubMed: 29149605]

(23). Black JW; Leff P Operational Models of Pharmacological Agonism. Proc. R. Soc. London, Ser. B 1983, 220, 141–162. [PubMed: 6141562]

(24). (a)Budzik B; Garzya V; Shi DC; Walker G; Woolley-Roberts M; Pardoe J; Lucas A; Tehan B; Rivero RA; Langmead CJ; Watson J; Wu Z; Forbes IT; Jin J Novel N-Substituted Benzimidazolones as Potent, Selective, CNS-Penetrant, and Orally Active M-1 mAChR Agonists. ACS Med. Chem. Lett 2010, 1, 244–248. [PubMed: 24900202] (b)Obase H; Takai H; Teranishi M; Nakamizo N Synthesis of (1-Substituted Piperidin-4-yl)-1H-benzimidazoles and (1-Substittued Piperidine-4-yl)-3,4-dihydroquinazolines as Possible Antihypertensive Agents. J. Heterocycl. Chem 1983, 20, 565–573.

(25). Kawamoto H; Ozaki S; Itoh Y; Miyaji M; Arai S; Nakashima H; Kato T; Ohta H; Iwasawa Y Discovery of the First Potent and Selective Small Molecule Opioid Receptor-like (ORL1) Antagonist: 1-[(3R4R)-1-Cylcooctylmethyl-3-hydroxymethyl-4-piperidyl]-3-ethyl-1,3-dihydro-2H-benzimidazole-2-one (J-113397). J. Med. Chem 1999, 42, 5061–5063. [PubMed: 10602690]

(26). Choi JY; Calvet CM; Gunatilleke SS; Ruiz C; Cameron MD; McKerrow JH; Podust LM; Roush WR Rational Development of 4-Aminopyridyl-based Inhibitors Targeting Trypanosoma cruzi CYP51 as Anti-chagas Agents. J. Med. Chem 2013, 56, 7651–7668. [PubMed: 24079662]

(27). Stahl EL; Zhou L; Ehlert FJ; Bohn LM A Novel Method for Analyzing Extremely Biased Agonism at G Protein–Coupled Receptors. Mol. Pharmacol 2015, 87, 866–877. [PubMed: 25680753]

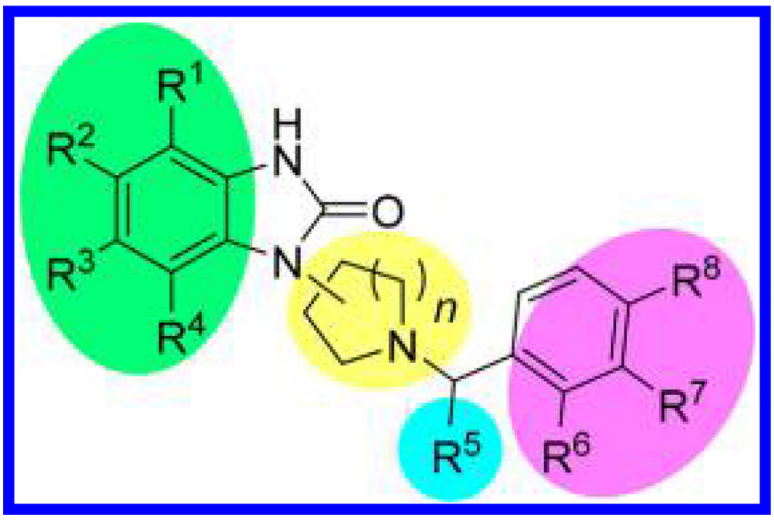

Figure 1.

General structure of *N*-benzyl piperidine 4-benzimidazolones. The sites for structure diversification R^1–R^8 and *n* are highlighted by the colored circles.

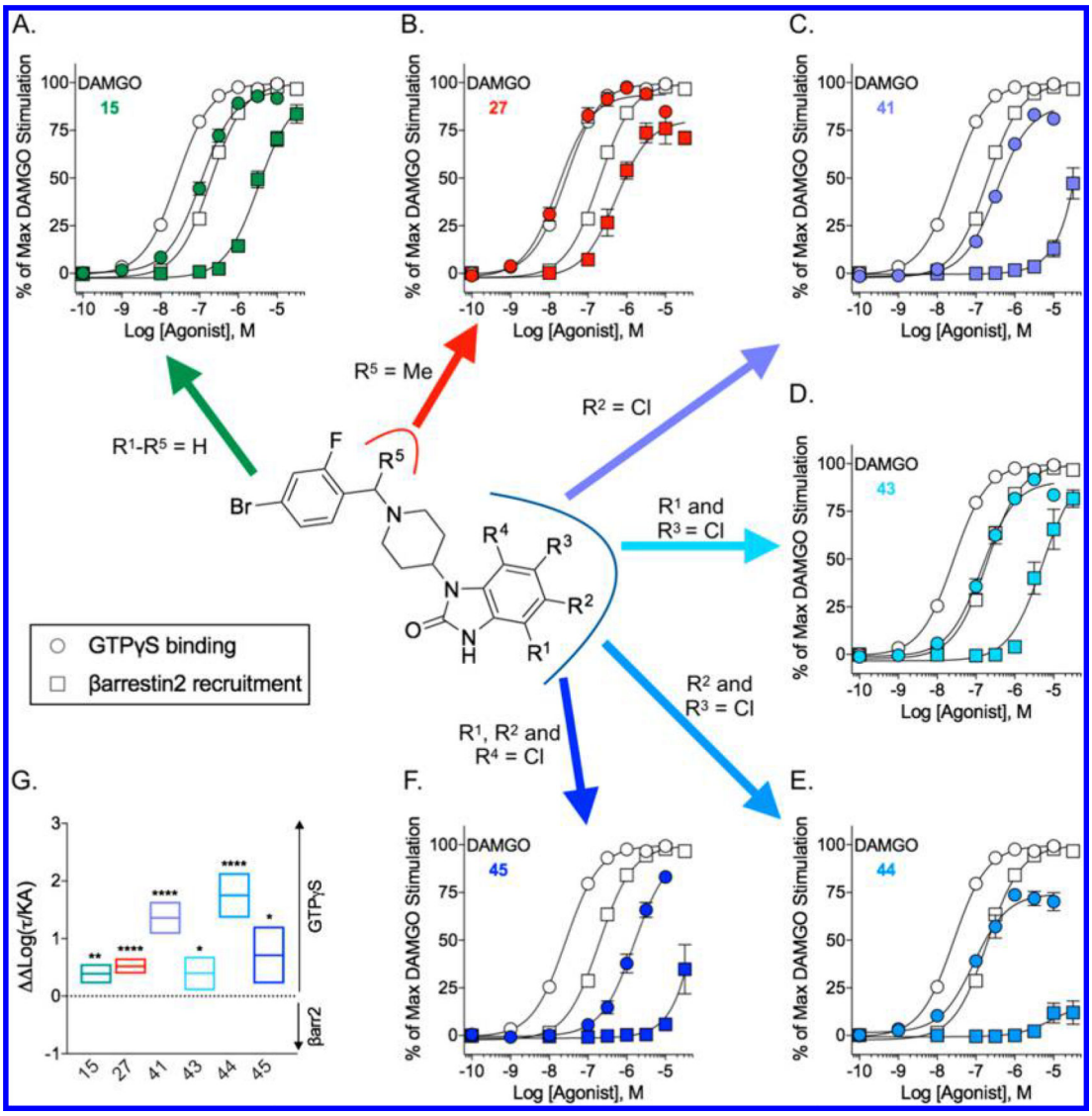

Figure 2.

SAR increasing activation of G protein binding with differential β-arrestin 2 signaling profiles. Four analogues were synthesized to determine how the addition of chlorine substituents to the benzimidazolone ring affects bias (**41, 43–45**). Analogues were compared to compound **15**, which has an unsubstituted benzimidazolone ring. Compound **27** was made to determine the effect that the addition of a benzylic methyl group had on bias compared to **15**. Concentration–response curves in the GTPγS binding (circles) and β-arrestin2-EFC assays (squares) are shown for the test compounds (solid symbols) versus DAMGO (open symbols) and are presented as mean ± SEM; curves are the result of three-parameter nonlinear regression analysis. $\Delta\Delta\log(\tau/K_A)$ values are plotted to demonstrate relative bias with 95% confidence intervals. Significant bias compared to DAMGO was determined by an unpaired, two-tailed *t* test: ****$p < 0.0001$; **$p < 0.01$; *$p < 0.05$.

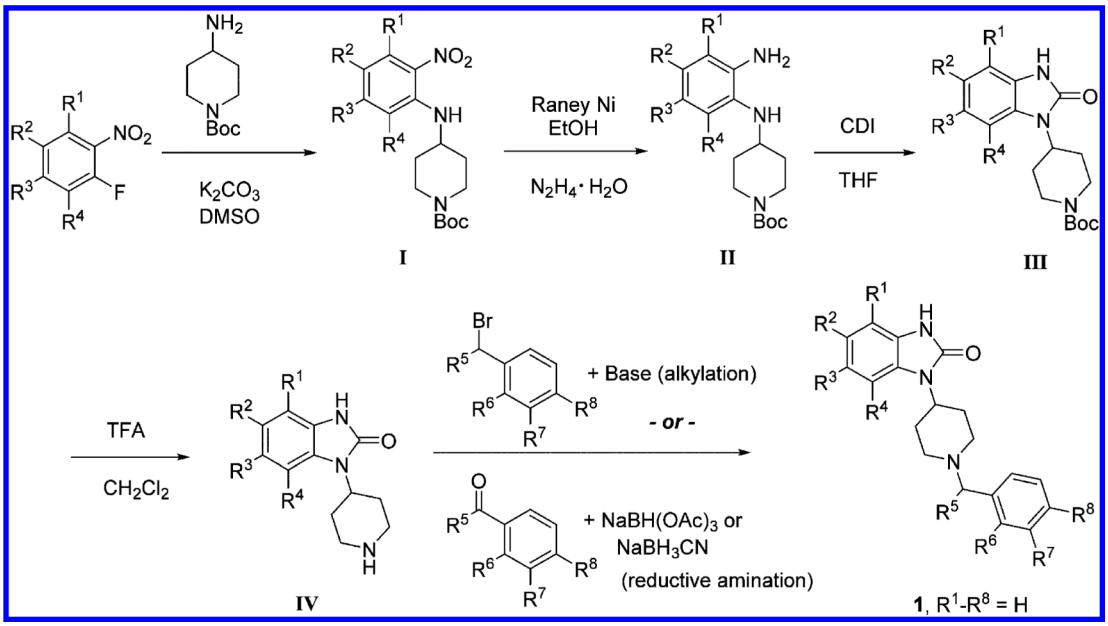

Scheme 1.

General Five-Step Synthetic Route for the Preparation of Substituted Piperidine 4-Benzimidazolones

J Med Chem. Author manuscript; available in PMC 2019 February 22.

Table 1.

GTPγS Binding and βarrestin2 Recruitment Activity of *N*-Benzyl Piperidine 4-Benzimidazolone Derivatives with *N*- Benzyl Substituents R^6–R^8.[a]

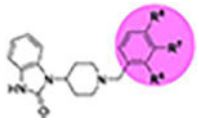				^{35}S-GTPγS Binding[b]			βarrestin2 Recruitment[b]			Bias (GTPγS/βarr2)	
Agonist	**R^6**	**R^7**	**R^8**	**EC_{50} (nM)**	**E_{MAX} (%)[c]**	**$\Delta\log(\tau/K_A)$**	**EC_{50} (nM)[c]**	**E_{MAX} (%)[c]**	**$\Delta\log(\tau/K_A)$**	**$\Delta\Delta\log(\tau/K_A)$ 95%(*CI*)[d]**	**Bias Factor**
DAMGO				33 ± 1	100		220 ± 8.3	100		0	1.0
Morphine				64 ± 3	83 ± 1	−0.3 ± 0.03	379 ± 17	24 ± 1	−0.6 ± 0.03	0.25 (0.17 to 0.33)[e]	1.8
1				2183 ± 290	78 ± 3	−1.8 ± 0.06	8255 ± 1676	40 ± 2	−1.8 ± 0.07	−0.04 (−0.25 to 0.16)	0.9
2	Cl			200 ± 19	92 ± 2	−0.8 ± 0.07	4487 ± 606	96 ± 9	−1.2 ± 0.05	0.4 (0.21 to 0.59)[f]	2.5
3		Cl		1354 ± 195	71 ± 1	−2 ± 0.06	>10,000[c]	10 ± 0.4[c]	−2.0 ± 0.09	0.22 (−0.08 to 0.52)	1.6
4[h]			Cl	551 ± 58	68 ± 4	−1.4 ± 0.09	7656 ± 1469	67 ± 10	−1.5 ± 0.08	0.07 (−0.25 to 0.39)	1.2
5			Me	433 ± 47	86 ± 2	−1.0 ± 0.06	2400 ± 497	63 ± 3	−1.1 ± 0.08	0.01 (−0.27 to 0.29)	1.0
6			Br	367 ± 37	76 ± 4	−1.2 ± 0.1	6611 ± 1076	77 ± 6	−1.3 ± 0.06	0.05 (−0.22 to 0.31)	1.1
7			OMe	591 ± 49	88 ± 3	−1.2 ± 0.05	2254 ± 303	41 ± 3	−1.2 ± 0.01	−0.04 (−0.45 to 0.36)	0.91
8			NHC(O)Me	760 ± 75	89 ± 6	−1.4 ± 0.04	3435 ± 889	29 ± 3	−1.4 ± 0.1	0.06 (−0.36 to 0.47)	1.1
9			CN	3424 ± 693	48 ± 2	−2.2 ± 0.1	NC[c]	1 ± 0.5[c]	/	/	/
10			$C(O)NH_2$	NC	7.7 ± 1[c]	/	NC[c]	0.03 ± 0.1[c]	/	/	/
11		OMe		1158 ± 160	33 ± 1	−1.9 ± 0.02	>10,000[c]	8 ± 1[c]	−2.2 ± 0.2	0.30 (−0.03 to 0.62)	2.0
12		OCF_3		1621 ± 183	64 ± 4	−1.8 ± 0.05	9326 ± 1738	29 ± 4	−1.8 ± 0.09	0.03 (−0.19 to 0.24)	1.1
13		Cl	Cl	6423 ± 565	27 ± 2	−2.8 ± 0.2	NC[c]	4 ± 3[c]	/	/	/
14	Me		Cl	152 ± 10	93 ± 1	−0.6 ± 0.03	2880 ± 411	75 ± 5	−1.2 ± 0.1	0.58 (0.30 to 0.87)[g]	3.8
15	F		Br	110 ± 16	96 ± 0.1	−0.7 ± 0.04	3357 ± 60	94 ± 6	−1.1 ± 0.04	0.39 (0.22 to 0.56)[g]	2.5

[a] If blank or not shown, R^X = H. "/" = not determined.

[b] Within each assay, potency (EC_{50}) and efficacy (E_{MAX}) values were calculated by nonlinear regression and $\Delta\log(\tau/K_A)$ values were determined by the operational model, relative to DAMGO. Data are presented as mean ± SEM of three or more assays run in duplicate or triplicate.

[c] In instances where the data did not converge to a nonlinear regression curve fitting due to not reaching plateau at the highest concentrations tested ($10^{-4.5}$ M in the β-arrestin assay, 10^{-5} M in the G protein assay), the EC_{50} is is noted as >10000 nM (if some stimulation could be observed) or NC (if the maximum concentration produced no effect) *and* the percentage of maximum stimulation at 10000 nM is provided rather than an E_{MAX} value where indicated.

[d] For $\Delta\Delta\log(\tau/K_A)$ values, 95% confidence intervals (95% CI) are provided. Significant bias compared to DAMGO was determined by an unpaired, two-tailed *t* test:

[e] $p < 0.0001$.

[f] $p < 0.001$.

[g] $p < 0.01$, otherwise $p > 0.05$.

[h] Compound **4** was previously reported as SR-20382.[22]

J Med Chem. Author manuscript; available in PMC 2019 February 22.

Table 2.

GTPγS Binding and βarrestin2 Recruitment Activity of *N*-Benzyl Piperidine 4-Benzimidazolone Derivatives with *N*- Benzyl Substituents R^5–R^8[a]

					^{35}S-GTPγS Binding[b]			βarrestin2 Recruitment[b]			Bias (GTPγS/βarr2)	
Agonist	**R^5**	**R^6**	**R^7**	**R^8**	**EC_{50} (nM)**	**E_{MAX} (%)**	**Δlog(τ/K_A)**	**EC_{50} (nM)**	**E_{MAX} (%)**	**Δlog(τ/K_A)**	**ΔΔlog(τ/K_A) 95%(CI)[c]**	**Bias Factor**
DAMGO					33 ± 1	100		220 ± 8.3	100		0	1.0
Morphine					64 ± 3	83 ± 1	−0.3 ± 0.03	379 ± 17	24 ± 1	−0.6 ± 0.03	0.25 (0.17 to 0.33)[d]	1.8
16[e]	Me				102 ± 10	89 ± 7	−0.5 ± 0.04	447 ± 52	67 ±4	−0.3 ± 0.07	−0.18 (−0.45 to 0.08)	0.7
17	Me	Cl			31 ± 0.21	96 ± 1	0.05 ± 0.05	199 ± 19	79 ± 15	0.1 ± 0.06	−0.01 (−0.2 to 0.18)	1.0
18[e]	Me			Cl	16 ± 1.2	97 ± 7	0.3 ± 0.07	184 ± 24	95 ± 4	0.02 ± 0.06	0.32 (0.09 to 0.56)[f]	2.1
19	Et			Cl	1593 ± 194	58 ± 1	−1.9 ± 0.08	6050 ± 1233	32 ± 4	−2 ± 0.08	−0.09 (−0.36 to 0.17)	0.81
20	Me			F	75 ± 8.3	93 ± 2	−0.4 ± 0.05	377 ± 76	78 ± 5	−0.2 ± 0.1	−0.26 (−0.53 to 0.02)	0.56
21	Me			Br	4.8 ± 0.41	91 ± 2	0.8 ± 0.02	182 ± 42	92 ± 5	0.2 ± 0.1	0.61 (0.11 to 1.11)[f]	4.1
22	Me			OMe	13 ± 0.64	95 ± 2	0.4 ± 0.03	87 ± 18	75 ± 8	0.4 ± 0.1	−0.06 (−0.50 to 0.37)	0.86
23	Me			OEt	189 ± 25	94 ± 2	−0.7 ± 0.06	1074 ± 165	50 ± 3	−0.6 ± 0.1	−0.04 (−0.33 to 0.24)	0.90
24	Me			O*i*Pr	399 ± 31	83 ± 2	−1.1 ± 0.06	5413 ± 373	33 ± 1	−1.6 ± 0.1	0.56 (0.22 to 0.90)[f]	3.6
25[e]	Me		-OCH_2CH_2O-		98 ± 8.5	77 ± 3.9	−0.5 ± 0.02	407 ± 50	59 ± 2.2	−0.2 ± 0.06	−0.32 (−0.45 to −0.2)[d]	0.47
26	Me			OCF_3	31 ± 4.7	96 ± 1	0.1 ± 0.08	1678 ± 328	100 ± 3	−0.8 ± 0.06	0.92 (0.64 to 1.20)[d]	8.3
27	Me	F		Br	18 ± 2.4	93 ± 2	0.2 ± 0.04	523 ± 67	82 ± 7	−0.4 ± 0.05	0.52 (0.39 to 0.66)[d]	3.3
28	Me	F		Cl	22 ± 2.1	98 ± 3	0.2 ± 0.04	484 ± 94	82 ± 6	−0.3 ± 0.09	0.46 (0.10 to 0.82)[f]	2.9

[a] If blank or not shown, R^X = H. All compounds were made and tested as racemates.

[b] Within each assay, potency (EC_{50}) and efficacy (E_{MAX}) values were calculated by nonlinear regression and Δlog(τ/K_A) values were determined by the operational model, relative to DAMGO. Data are presented as mean ± SEM of three or more assays run in duplicate or triplicate.

[c] For ΔΔlog(τ/K_A) values, 95% confidence intervals (95% *CI*) are provided. Significant bias compared to DAMGO was determined by an unpaired, two-tailed *t* test.

[d] $p < 0.0001$.

[e] Compounds **16**, **18**, and **25** were previously reported as (±)SR-8595, (±)SR-11065, and (±)SR-11501, respectively.[22]

J Med Chem. Author manuscript; available in PMC 2019 February 22.

Table 3.

GTPγS Binding and βarrestin2 Recruitment Activity of *N*-Benzyl Piperidine 4-Benzimidazolone Derivatives with Benzimidazolone Substituents R^1–R^4[a]

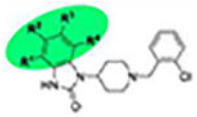					^{35}S-GTPγS Binding[b]			βarrestin2 Recruitment[b]			Bias (GTPγS/βarr2)	
Agonist	**R^1**	**R^2**	**R^3**	**R^4**	**EC_{50} (nM)**	**E_{MAX} (%)[c]**	**Δlog(τ/K_A)**	**EC_{50} (nM)**	**E_{MAX} (%)[c]**	**Δlog(τ/K_A)**	**ΔΔlog(τ/K_A) 95%(CI)[d]**	**Bias Factor**
DAMGO					33 ± 1	100		220 ± 8.3	100		0	1.0
Morphine					64 ±3	83 ± 1	−0.3 ± 0.03	379 ± 17	24 ± 1	−0.6 ± 0.03	0.25 (0.17 to 0.33)	1.8
2					200 ± 19	92 ± 2	−0.8 ± 0.07	4487 ± 606	96 ± 9	−1.2 ± 0.05	0.4(0.21 to 0.59)	2.5
29	Cl				48 ± 6.7	99 ± 1	−0.1 ± 0.09	1962 ± 326	69 ± 10	−0.9 ± 0.08	0.76(0.51 to 1.01)	5.8
30		Cl			184 ± 23	93 ± 2	−0.7 ± 0.09	>10,000	47 ± 4[c]	−1.6 ± 0.06	0.85 (0.60 to 1.11)	7.1
31			Cl		I48± 16	99 ± 2	−0.6 ± 0.08	>10,000	40 ± 4[c]	−1.5 ± 0.2	0.84 (0.46 to 1.22)	6.9
32				Cl	3109 ± 747	66 ± 16	−2.2 ± 0.07	NC	1 ± 1[c]	/	/	/
33		Me			224 ± 9.6	99 ± 2	−0.8 ± 0.03	6769 ± 1337	79 ± 4	−1.5 ± 0.05	0.65 (0.49 to 0.81)	4.5
34		Br			57 ± 5	97 ± 2	−0.4 ± 0.04	843 ± 31	80 ± 3	−0.5 ± 0.03	0.12 (−0.03 to 0.27)	1.3
35		F			111 ± 16	96 ± 1	−0.7 ± 0.1	1644 ± 315	78 ± 6	−0.8 ± 0.09	0.11 (−0.26 to 0.47)	1.3
36		OMe			2123 ± 76	103 ± 3	−1.9 ± 0.01	> 10,000	18 ± 2[c]	−2.2 ± 0.1	0.28 (−0.17 to 0.73)	1.9
37		OCF_3			1236 ± 111	57 ± 1	−1.9 ± 0.03	NC	3 ± 1[c]	/	/	/
38		SO_2Me			7618 ± 737	75 ± 7	−2.5 ± 0.07	>10,000	6 ± 1[c]	−2.5 ± 0.04	0.01 (−0.15 to 0.17)	1.0
39		CN			>10,000	17 ± 2[c]	−2.8 ± 0.06	NC	−0.2 ± 0.2[c]	/	/	/

[a] If blank or not shown, R^X = H. "/" = not determined.

[b] Within each assay, potency (EC_{50}) and efficacy (E_{MAX}) values were calculated by nonlinear regression and Δlog(τ/K_A) values were determined by the operational model, relative to DAMGO. Data are presented as mean ± SEM of three or more assays run in duplicate or triplicate.

[c] In instances where the data did not converge (NC) and therefore no potency value could be calculated, or produced a value outside the experimental range (EC_{50} > 10000 nM), the percentage of maximum stimulation at 10,000 nM is provided.

[d] For ΔΔlog(τ/K_A) values, 95% confidence intervals (95% CI) are provided. Significant bias compared to DAMGO was determined by an unpaired, two-tailed *t* test.

[e] $p < 0.0001$.

[f] $p < 0.001$.

[g] $p < 0.01$, otherwise $p > 0.05$.

Table 4.

GTPγS Binding and βarrestin2 Recruitment Activity of *N*-Benzyl Piperidine 4-Benzimidazolone Derivatives with Benzimidazolone Substituents R^1–R^5[a]

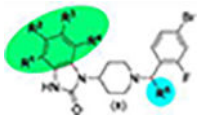						^{35}S-GTPγS Binding[c]			βarrestin2 Recruitment[c]			Bias (GTPγS/βarr2)	
Agonist	**R^1**	**R^2**	**R^3**	**R^4**	**R^5**	**EC_{50}(nM)**	**E_{MAX}(%)[d]**	**Δlog(τ/K_A)**	**EC_{50}(nM)**	**E_{MAX}(%)[d]**	**Δlog(τ/K_A)**	**ΔΔlog(τ/K_A) (95% CI)[e]**	**Bias Factor**
DAMGO						33 ± 1	100		220 ± 8.3	100		0	1.0
Morphine						64 ± 3	83 ± 1	−0.3 ± 0.03	379 ± 17	24 ± 1	−0.6 ± 0.03	0.25 (0.17 to 0.33)[f]	1.8
15						110 ± 16	96 ± 0.06	−0.7 ± 0.04	3357 ± 60	94 ±6	−1.1 ± 0.04	0.39 (0.22 to 0.56)[g]	2.5
27					Me[b]	18 ± 2.4	93 ± 2	0.2 ± 0.04	523 ± 67	82 ± 7	−0.4 ± 0.05	0.52 (0.39 to 0.66)[f]	3.3
40	Cl					55 ± 8.1	93 ± 2	−0.5 ± 0.1	2912 ± 189	71 ± 6	−1.1 ± 0.1	0.59 (0.21 to 0.98)[h]	3.9
41		Cl				355 ± 26	89 ± 2	−1.1 ± 0.04	>10,000	14 ± 4[d]	−2.5 ± 0.2	1.36(1.08 to 1.64)[f]	**23**
42			Cl			127 ± 11	88 ± 7	−0.6 ± 0.07	3459 ± 634	49 ± 9	−1.3 ± 0.1	0.62(0.31 to 0.94)[g]	4.2
43	Cl		Cl			153 ± 32	91 ± 2	−0.9 ± 0.1	>10,000	66 ± 10[d]	−1.3 ± 0.02	0.40 (0.10 to 0.69)[h]	2.5
44		Cl	Cl			91 ± 5.5	74 ± 4	−0.6 ± 0.06	>10,000	12 ± 5[d]	−2.4 ± 0.1	1.75 (1.36 to 2.14)[f]	**56**
45	Cl	Cl		Cl		1764 ± 384	99 ± 3	−1.8 ± 0.1	>10,000	5.9 ± 3[d]	−2.5 ± 0.06	0.71 (0.22 to 1.21)[h]	5.2

[a] If blank or not shown, R^X = H.

[b] Compounds were made and tested as racemates.

[c] Within each assay, potency (EC_{50}) and efficacy (E_{MAX}) values were calculated by nonlinear regression and Δlog(τ/K_A) values were determined by the operational model, relative to DAMGO. Data are presented as mean ± SEM of three or more assays run in duplicate or triplicate.

[d] In instances where the data produced a value outside the experimental range (EC_{50} > 10000 nM), the percentage of maximum stimulation at 10000 nM is provided.

[e] For Δlog(τ/K_A) values, 95% confidence intervals (95% CI) are provided. Significant bias compared to DAMGO was determined by an unpaired, two-tailed *t* test.

[f] $p < 0.0001$.

[g] $p < 0.01$

[h] $p < 0.05$.

Table 5.

GTPγS Binding and βarrestin2 Recruitment Activity of *N*-Benzyl Benzimidazolone Derivatives

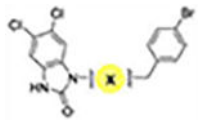		^{35}S-GTPγS Binding[a]			βarrestin2 Recruitment[a]			Bias (GTPγS/βarr2)	
Agonist	**X**	**EC_{50}(nM)**	**E_{MAX}(%)[b]**	**Δlog(τ/K_A)**	**EC_{50}(nM)**	**E_{MAX}(%)[b]**	**Δlog(τ/K_A)**	**ΔΔlog(τ/K_A) (95% CI)[c]**	**Bias Factor**
DAMGO		33 ± 1	100		220 ± 8.3	100		0	1.0
Morphine		64 ± 3	83 ± 1	−0.3 ± 0.03	379 ± 17	24 ± 1	−0.6 ± 0.03	0.25 (0.17 to 0.33)[d]	1.8
46[e]	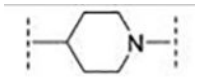	149 ± 9.1	83 ± 4	−0.8 ± 0.04	>10,000	3.6 ± 1[b]	−2.4 ± 0.04	1.66 (1.53 to 1.79)[d]	**45**
47	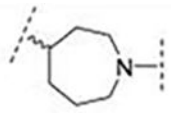	1403 ± 225	90 ± 9	−1.7 ± 0.05	>10,000	6.7 ± 4[b]	−2.6 ± 0.2	0.93 (0.31 to 1.55)[f]	8.5
48	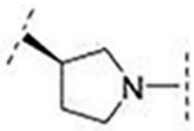	2975 ± 400	87 ± 6	−1.9 ± 0.07	>10,000	7.5 ± 3[b]	−2.7 ± 0.09	0.79(0.51 to 1.07)[d]	6.2
49	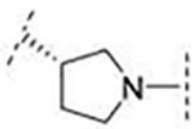	373 ± 31	90 ± 4	−1.1 ±0.08	>10,000	29 ± 6[b]	−1.8 ±02	0.73 (0.34 to 1 11)[g]	5.3
50	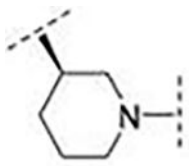	>10,000	24 ± 6[b]	−2.7 ± 0.4	NC	−0.3 ± 0.1[b]	/	/	/

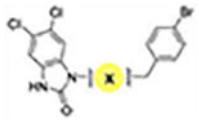		^{35}S-GTPγS Binding[a]			βarrestin2 Recruitment[a]			Bias (GTPγS/βarr2)	
Agonist	**X**	**EC_{50}(nM)**	**E_{MAX}(%)[b]**	**Δlog(τ/K_A)**	**EC_{50}(nM)**	**E_{MAX}(%)[b]**	**Δlog(τ/K_A)**	**ΔΔlog(τ/K_A) (95% CI)[c]**	**Bias Factor**
51	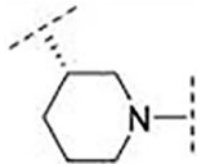	>10,000	21 ± 10[b]	−2.8 ± 0.08	NC	−0.3 ± 0.2	/	/	/

[a] Within each assay, potency (EC_{50}) and efficacy (E_{MAX}) values were calculated by nonlinear regression and Δlog(τ/K_A) values were determined by the operational model, relative to DAMGO. Data are presented as mean ± SEM of three or more assays run in duplicate or triplicate.

[b] In instances where the data did not converge (NC) or produced a value outside the experimental range (EC_{50} > 10000 nM), the percentage of maximum stimulation at 10000 nM is provided.

[c] For ΔΔlog(τ/K_A) values, 95% confidence intervals (95% CI) are provided. Significant bias compared to DAMGO was determined by an unpaired, two-tailed *t* test:

[d] $p < 0.0001$.

[e] Compound **46** was previously reported as SR-15099.[22]

[f] $p < 0.05$.

[g] $p < 0.01$.

"/" = not determined

Table 6.

In Vitro and in Vivo Evaluation of Select *N*-Benzyl Piperidine 4-Benzimidazolone Derivatives[d]

Agonist	Structure[a]	^{35}S-GTPγS EC_{50} (nM)[b]	BiasFactor	CP450 Inhibition % Inhibition at 10 μM				Microsome Stability $T_{1/2}$ life (minutes)		Brain Level (μM)[c]
				1A2	2C9	2D6	3A4	Human	Mouse	
Morphine	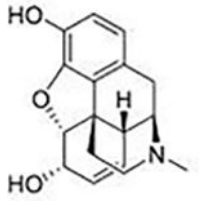	64	1.8							0.39 ± 0.07
25[d]	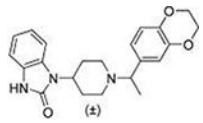	98	0.47	6	−30	−3	3	16	1	0.70 ± 0.16
26	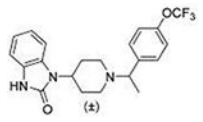	31	8.3	−40	1	−34	−46	120	14	
29	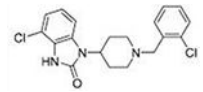	48	5.8	40	55	50	13	8	3	
30	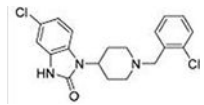	184	7.1	−23	20	38	−2	6	3	
31	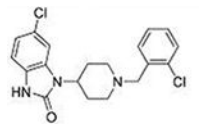	148	6.9	12	34	41	0	17	4	

Agonist	Structure[a]	^{35}S-GTPγS EC_{50} (nM)[b]	BiasFactor	CP450 Inhibition % Inhibition at 10 μM				Microsome Stability $T_{1/2}$ life (minutes)		Brain Level (μM)[c]
				1A2	2C9	2D6	3A4	Human	Mouse	
41	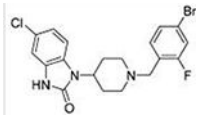	355	23	4	41	18	17	84	17	17 ± 0.35
44	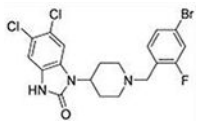	91	56	−10	−1	−16	−16	73	31	4.6 ± 0.28
46[d]	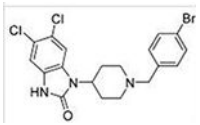	149	45	5	14	−1	−3	233	35	11 ± 2.2

[a] Compounds **25** and **26** were made and tested as racemates.

[b] Data are presented as mean ± SEM of three or more assays run in duplicate or triplicate.

[c] Compounds **25** and **46** were previously reported as (±)SR-11501 and SR-15099, respectively.[22]

[d] Microsomal stability assays were conducted in vitro. Brain levels of compound were determined in mice 1 h following a 6 mg/kg, ip injection of the compound indicated.